

Fabrication and Performance of All-Solid-State Li–Air Battery with SWCNTs/LAGP Cathode

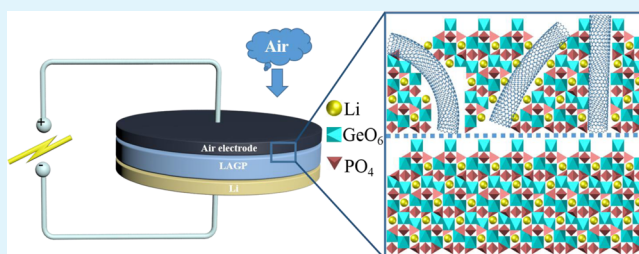
Yijie Liu,[†] Bojie Li,[†] Hirokazu Kitaura,[‡] Xueping Zhang,[†] Min Han,[†] Ping He,^{*,†} and Haoshen Zhou^{*,†,‡}

[†]College of Engineering and Applied Sciences and Collaborative Innovation Center of Advanced Microstructures, National Laboratory of Solid State Microstructures, Nanjing University, Nanjing, 210093, China

[‡]Energy Technology Research Institute, National Institute of Advanced Industrial Science and Technology (AIST), Umezono 1-1-1, Tsukuba, 305-8568, Japan

Supporting Information

ABSTRACT: The all-solid-state Li–air battery has been fabricated, which is constructed by a lithium foil anode, a NASICON-type solid state electrolyte $\text{Li}_{1+x}\text{Al}_y\text{Ge}_{2-y}(\text{PO}_4)_3$ (LAGP) and single-walled carbon nanotubes (SWCNTs)/LAGP nanoparticles composite as air electrode. Its electrochemical performance was investigated in air atmosphere. Particularly, this battery exhibited a larger capacity about 2800 mAh g^{-1} for the first cycle, while comparatively the battery with multiwalled carbon nanotubes (MWCNTs)/LAGP as cathode had a capacity of only about 1700 mAh g^{-1} . Also, the battery with SWCNTs/LAGP showed improved cycling performance with a reversible capacity of 1000 mAh g^{-1} at a current density of 200 mA g^{-1} . Our result demonstrated that the all-solid-state Li–air battery with SWCNTs/LAGP as cathode catalyst has a considerable potential for practical application.



KEYWORDS: all-solid-state, Li–air batteries, solid-state electrolyte, SWCNTs, air electrode catalyst

The Li–air battery has attracted worldwide attention because of its extremely high theoretical energy density, according to the reactions of lithium peroxide's forming and deforming ($2\text{Li} + \text{O}_2 \leftrightarrow \text{Li}_2\text{O}_2$). After the pioneering work of the Li–air battery in 1996, intensive works are mainly focused on the research of nonaqueous Li–air batteries with a typical structure of Li anode/organic electrolyte/air electrode.¹ However, there remain many problems related to nonaqueous Li–air batteries, among which some arise from the application of organic liquid electrolytes.^{2–5} For example, the decomposition of alkyl carbonate electrolyte during discharging resulted in the formation of undesirable reactants, which accumulated on the surface of the cathode and finally resulted in the deterioration of battery performance.³ Besides, this kind of battery has safety hazards owing to the flammable and toxic properties of liquid organic electrolyte. To solve this problem, inorganic solid state electrolytes are introduced into the structure of Li–air batteries.^{6–11} Substituting inorganic electrolyte for organic solid electrolytes can avoid side reactions caused by organic electrolytes during electrochemical process. Moreover, inorganic solid electrolytes can effectively protect Li metal anode from CO_2 and H_2O in ambient air, and nonvolatile solid electrolyte seems more applicable to long-term use than liquid electrolyte.

Our previous work reported an all-solid-state Li–air battery with the structure of Li metal anode, a double-layer electrolyte containing a polymer electrolyte and an inorganic solid electrolyte, and an air electrode composed of MWCNTs and

solid electrolyte particles.¹⁰ In this work, the polymer membrane was used to avoid LATP directly contacting with Li metal, in order to protect Ti^{4+} from being reduced to Ti^{2+} by lithium. However, the additional polymer electrolyte introduced interfacial resistances between Li/polymer and polymer/LATP and it also increased the total resistance of the cell. Thus, further optimized designs for the all-solid-state Li–air battery abandon the buffering polymer membrane, and, instead, an inorganic solid state electrolyte is directly attached to Li metal.¹¹ Here, the inorganic solid-state electrolyte is supposed to be chemically stable against the reaction with Li metal. NASICON-type material lithium aluminum germanium phosphate ($\text{Li}_{1+x}\text{Al}_y\text{Ge}_{2-y}(\text{PO}_4)_3$, LAGP) has received considerable attention as solid state electrolytes for secondary lithium batteries.^{12–14} In the LAGP ceramics, Al^{3+} substitution for Ge^{4+} introduces additional lithium in the structure and improves the total lithium ion conductivities. In addition, the LAGP ceramics exhibit good and relative stability in air atmosphere and in contact with Li metal, respectively. Moreover, LAGP has an electrochemical window as high as 6 V (vs Li/Li^+).¹⁴ On the basis of the high lithium ion conductivity, wide electrochemical window, good chemical stability in air, and relative chemical stability against lithium, LAGP ceramics are very applicable to fabricating all-solid-state Li–air batteries with superior electro-

Received: May 21, 2015

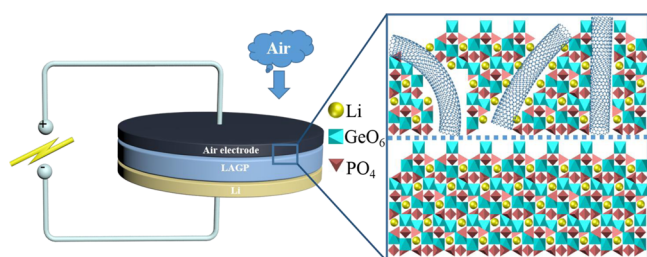
Accepted: July 15, 2015

Published: July 15, 2015

chemical performance. From this point of view, another all-solid-state Li–air battery with the structure of Li anode, LAGP solid-state electrolyte and composite cathode consisting of MWCNTs and LAGP nanoparticles was fabricated. This battery showed relative small resistance and much improved electrochemical performance compared with the aforementioned battery. In this paper, we constructed a composite air electrode composed of single-walled carbon nanotubes and LAGP nanoparticles. SWCNTs are known as good electronic conductors with large surface area (see Supporting Information Figure S1) and have been investigated as cathode catalysts in nonaqueous Li–air batteries.^{15–19} Besides, it has been reported that SWCNTs are prone to adsorb oxygen and hence have higher electrical conductance, which may improve the electrochemical performance of the cell.¹⁶ Moreover, SWCNTs have a better crystallinity and less defects compared with MWCNTs, which can reduce side reactions during electrochemical processes. As a result, SWCNTs are supposed to be properly mixed with LAGP nanoparticles, in order to provide mixing channels for electrons and lithium ions.^{7–11}

The all-solid-state Li–air battery was assembled by following procedures. The NASICON-type lithium ion conductor $\text{Li}_{1.5}\text{Al}_{0.5}\text{Ge}_{1.5}(\text{PO}_4)_3$ was synthesized by a conventional solid-state reaction.¹¹ The powder of LAGP was pressed into a pellet with a diameter of 19 mm and a thickness of about 1.0 mm. This pellet was sintered at 900 °C for 6 h. The calculated total lithium ionic conductivity of the sintered LAGP ceramic was about 2×10^{-4} S/cm (See Supporting Information Figure S2). The air electrode was constructed on one side of the pellet as follows. SWCNTs and LAGP nanoparticles with a weight ratio of 10–100 were high-energy ball milled at a rate of 700 rpm for 2 h, and then dispersed into solution composed of 5% polyvinylidene fluoride and 95% *N*-methyl-2-pyrrolidone. The solution was uniformly painted on one side of LAGP pellet and heated at 700 °C for 10 min in Ar atmosphere. The mass of the air electrode was about 0.5 mg. An Al mesh was used as the current collector. The lithium metal was first melted and then thermally adhered with a Cu current collector to the other side of the LAGP ceramic pellet as the anode. Scheme 1 presents a

Scheme 1. Schematic Representation of the Proposed All-Solid-State Li–Air Battery Using Li Anode, LAGP Ceramic Electrolyte, and an Air Electrode Composed of SWCNTs and LAGP Particles^a



^aThe yellow spheres represent Li metal; the red tetrahedral represent PO_4 ; and the cyan octahedral represent GeO_6 .

schematic diagram of the proposed all-solid-state Li–air battery. In the battery, the composite electrode is exposed to air atmosphere, while other parts of the battery are actually sealed by a plastic film to avoid the influence of air. In this work, the electrochemical performance of the all-solid-state Li–air battery was all investigated in air.

Figure 1 shows the TEM pattern of SWCNTs incorporated with LAGP nanoparticles in the range of 100–200 nm. It is

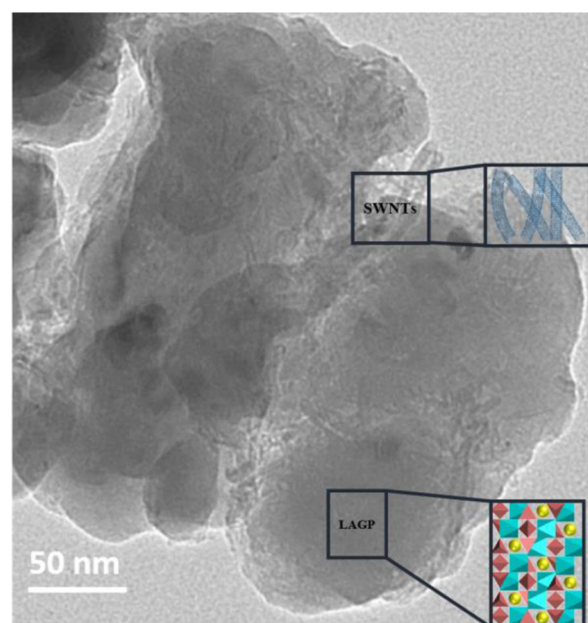


Figure 1. TEM image of the air electrode SWCNTs and LAGP nanoparticles in the all-solid-state Li–air battery. The scale bar was 50 nm.

revealed that the SWCNTs are distributed closely on the LAGP particle surface. The solid electrolyte LAGP was confirmed by the Rietveld refinement of XRD pattern in Supporting Information Figure S3. The diffraction peaks corresponding to $\text{LiGe}_2(\text{PO}_4)_3$ phase were observed, which can be attributed to the similar ionic radii of Ge^{4+} and Al^{3+} . The LAGP nanoparticles were used as lithium ion conduction paths incorporated with SWCNTs, which provide channels for electron conduction.

As shown in Figure 2, it can be clearly seen that the all-solid-state Li–air battery with SWCNTs/LAGP has got a larger specific capacity about 2800 mAh g^{-1} compared with that containing MWCNTs/LAGP, which may be attributed to the good electronic properties and large surface area of SWCNTs.

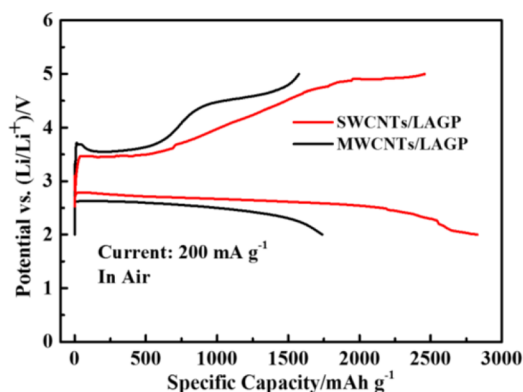


Figure 2. First discharge–charge curves of all-solid-state Li–air batteries with SWCNTs/LAGP and MWCNTs/LAGP as air electrodes at a current density of 200 mA g^{-1} according to weight of SWCNTs or MWCNTs, and the cutoff voltages were set as 2 V for discharging and 5 V for charging.

Moreover, on discharging, the battery with SWCNTs/LAGP had a plateau about 2.7 V, and its discharging overpotential was obviously smaller than that with MWCNTs/LAGP, which seems to be related to the good ORR catalytic behavior of SWCNTs. On charging, the curves can be cut into three parts. The first part had a plateau at 3.45 V below 500 mAh g⁻¹, and then it slowly increased to 4.9 V when at the same time the capacity reached about 2000 mAh g⁻¹. Correspondingly, the two parts were believed to be related to the oxidation of the LiOH (hydration) and Li₂O₂.^{18,19} Since the air electrode was exposed to ambient air, it cannot be avoided that the LiOH and Li₂O₂ reacted with CO₂ to form Li₂CO₃. Therefore, for the third part with a platform at about 4.9 V, it was considered to be related to the oxidation of Li₂CO₃.

The first discharge and charge curves with a specific capacity of 1000 mAh g⁻¹ at a current density of 400 mA g⁻¹ (according to the mass of SWCNTs) were presented in Figure 3a, where

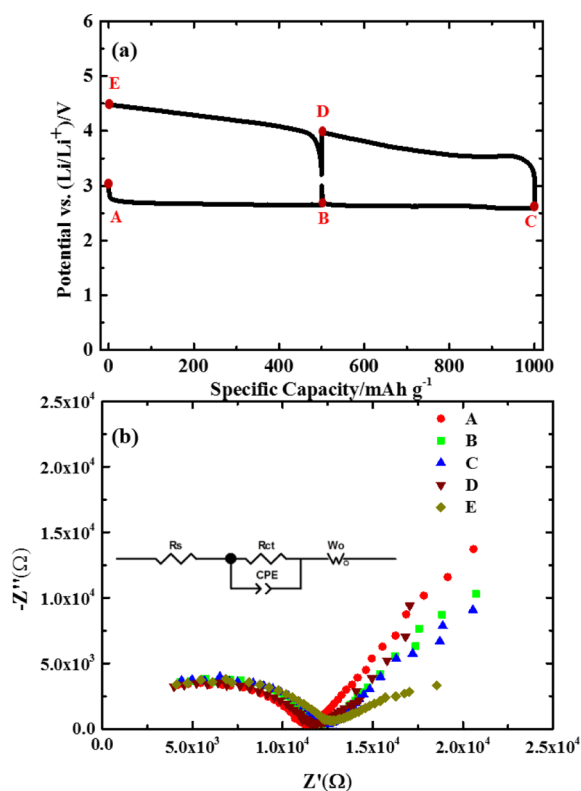


Figure 3. (a) First charge and discharge curves at a current density of 400 mA g⁻¹ and (b) electrochemical impedance spectra of the all-solid-state Li–Air battery at points from A to E. The frequency range was 0.1 to 105 Hz and the applied voltage was 5 mV. The inset shows the equivalent circuit.

the discharge curve had a plateau of about 2.65 V. The charge curve first increased from 3.2 to 3.5 V, and then slowly charged to about 4.5 V. On contrast, two obvious plateaus were observed when LAGP and MWCNTs were used as components of the air electrode in our previous work.¹¹ It is suggested that SWCNTs with better crystallinity and less defects may have less side reactions compared with MWCNTs and, as a result, no obvious two plateaus were noticed. Besides, the electrochemical impedance spectra (EIS) were investigated when the cell was discharged to two depths (B and C), 500 and 1000 mAh g⁻¹, respectively. In Figure 3b, the impedance spectra showed that only one semicircle was observed in high

frequency and by fitting the data with an equivalent circuit, where R_{ct} represented the charge transfer resistance and it slightly increased the cell resistance during discharge. The fitting data of R_{ct} was presented in Supporting Information Table S1. Then, the cell was recharged to two depths (D and E), 500 and 1000 mAh g⁻¹, respectively. When charged to 500 mAh g⁻¹, there was little change in the cell resistance and only one semicircle was observed. Similar behavior was also presented in point E. This suggested that the air electrode was relatively stable, which can be attributed to the better crystallinity and good catalytic property of SWCNTs.

To investigate the cycling performance of the all-solid-state Li–air battery. The cell was discharged and charged between 2.0 and 5.0 V under a current density of 400 mA g⁻¹, and the capacity was limited to 1000 mAh g⁻¹. Figure 4a depicts the

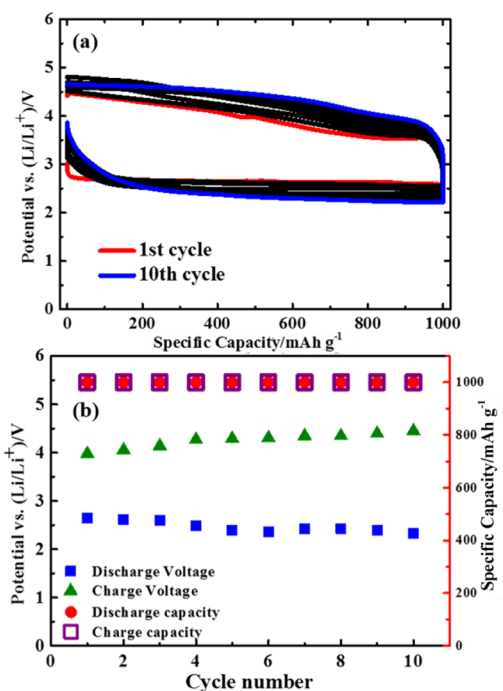


Figure 4. Cycle performance of the all-solid-state Li–Air battery. (a) Discharge and charge curves under a capacity limitation of 1000 mAh g⁻¹ for 10 cycles at a current of 400 mA g⁻¹ and (b) average voltages of the charge and discharge curves.

cycle profiles of the cell, which was recharged over 10 cycles. The superior cycling performance of the cell may be related to the good electronic properties and large surface area of the SWCNTs.^{15,16} Besides, the well-integrated tunnels for both electrons and ions of the composite air electrode were also important for the improved performance.^{7–11} Last but not the least, the presence of H₂O in air atmosphere, which enhanced the electronic conductance and contributed to the improved electrochemical process.^{20,21} Moreover, it is exhibited in Figure 4b that the discharge curves had a plateau at about 2.65 V for the first cycle, which had an average charging voltage of about 3.97 V. Then, with the cell cycling, the discharging voltage decreased gradually from 2.65 to 2.32 V. Interestingly, the terminal of charge curves first increased and reached a maximum value of about 4.8 V at the fourth cycle. Later it decreased to only 4.65 V at the tenth cycle. However, the overpotentials of discharge and charge processes both slowly

increased, which may be attributed to accumulation of Li_2CO_3 on the surface of the cathode due to the exposure to air.

CONCLUSION

In summary, we proposed an all-solid-state Li–air battery composed of a Li metal foil anode, a NASICON-type solid electrolyte LAGP, and SWCNTs/LAGP as air electrode. The good electronic properties, large surface area and better crystallinity of SWCNTs benefit the electrochemical process. This all-solid-state Li–air battery showed a larger capacity of 2800 mAh g^{-1} for the first cycle discharge than that with MWCNTs/LAGP. The cell exhibited a good cycling performance with a limited capacity of 1000 mAh g^{-1} at a current density of 400 mA g^{-1} . However, because of the influence of CO_2 and H_2O , the electrochemical process in air atmosphere may be largely different with that in pure oxygen atmosphere. Obviously, the air electrode also needs to be further optimized in order to construct a three-dimensional network and more effective catalysts suitable for all-solid-state Li–air batteries are equally required.

ASSOCIATED CONTENT

Supporting Information

Nitrogen adsorption–desorption isotherm of SWCNTs and MWCNTs, electrochemical impedance spectra of the LAGP pellet, and Rietveld refinement of XRD pattern of LAGP. The Supporting Information is available free of charge on the ACS Publications website at DOI: 10.1021/acsami.5b04409.

AUTHOR INFORMATION

Corresponding Authors

*Email: pinghe@nju.edu.cn.

*E-mail: hszhou@nju.edu.cn.

Notes

The authors declare no competing financial interest.

ACKNOWLEDGMENTS

This work was partially supported financially by the National Basic Research Program of China (973 Program) (2014CB932302, 2014CB932303), National Natural Science Foundation of China (21373111, 21403107), and Natural Science Foundation of Jiangsu Province of China (BK2012309, BK20140055).

REFERENCES

- (1) Abraham, K. M.; Jiang, Z. A Polymer Electrolyte-Based Rechargeable Lithium/Oxygen Battery. *J. Electrochem. Soc.* **1996**, *143*, 1–5.
- (2) Li, F. J.; Zhang, T.; Zhou, H. S. Challenges of Non-aqueous Li–O₂ Batteries: Electrolytes, Catalysts, and Anodes. *Energy Environ. Sci.* **2013**, *6*, 1125–1141.
- (3) Freunberger, S. A.; Chen, Y. H.; Peng, Z. Q.; Griffin, J. M.; Hardwick, L. J.; Barde, F.; Novak, P.; Bruce, P. G. Reactions in the Rechargeable Lithium–O₂ Battery with Alkyl Carbonate Electrolytes. *J. Am. Chem. Soc.* **2011**, *133*, 8040–8047.
- (4) Chen, Y. H.; Freunberger, S. A.; Peng, Z. Q.; Barde, F.; Bruce, P. G. Li–O₂ Battery with A Dimethylformamide Electrolyte. *J. Am. Chem. Soc.* **2012**, *134*, 7952–7957.
- (5) Su, D.; Dou, S. X.; Wang, G. X. Gold Nanocrystals with Variable Index Facets as Highly Effective Cathode Catalysts for Lithium–Oxygen Batteries. *NPG Asia Mater.* **2015**, *7*, e155.
- (6) Zhou, H. S.; Wang, Y. G.; Li, H. Q.; He, P. The Development of a New Type of Rechargeable Batteries Based on Hybrid Electrolytes. *ChemSusChem* **2010**, *3*, 1009–1019.

(7) Kichambare, P.; Rodrigues, S.; Kumar, J. Mesoporous Nitrogen-Doped Carbon-Glass Cathodes for Solid-State Lithium–Oxygen batteries. *ACS Appl. Mater. Interfaces* **2012**, *4*, 49–52.

(8) Kumar, B.; Kumar, J. Cathodes for Solid-State Lithium–Oxygen Cells: Roles of Nasicon Glass-Ceramics. *J. Electrochem. Soc.* **2010**, *157*, A611–A616.

(9) Kumar, B.; Kumar, J.; Leese, R.; Fellner, J.; Rodrigues, S.; Abraham, K. M. A Solid-State, Rechargeable, Long Cycle Life Lithium–Air Battery. *J. Electrochem. Soc.* **2010**, *157*, A50–A54.

(10) Kitaura, H.; Zhou, H. S. Electrochemical Performance of Solid-State Lithium–Air Batteries Using Carbon Nanotube Catalyst in the Air Electrode. *Adv. Energy Mater.* **2012**, *2*, 889–894.

(11) Kitaura, H.; Zhou, H. S. Electrochemical Performance and Reaction Mechanism of All-Solid-State Lithium–Air Batteries Composed of Lithium, $\text{Li}_{1+x}\text{Al}_y\text{Ge}_{2-y}(\text{PO}_4)_3$ Solid Electrolyte and Carbon Nanotube Air Electrode. *Energy Environ. Sci.* **2012**, *5*, 9077–9084.

(12) Aono, H.; Sugimoto, E.; Sadaoka, Y.; Imanaka, N.; Adachi, G. Y. Electrical Properties and Sinterability for Lithium Germanium Phosphate $\text{Li}_{1+x}\text{M}_x\text{Ge}_{2-x}(\text{PO}_4)_3$, M=Al, Cr, Ga, Fe, Sc, and in Systems. *Bull. Chem. Soc. Jpn.* **1992**, *65*, 2200–2204.

(13) Fu, J. Fast Li⁺ Ion Conducting Glass-Ceramics on the System $\text{Li}_2\text{O}-\text{Al}_2\text{O}_3-\text{GeO}_2-\text{P}_2\text{O}_5$. *Solid State Ionics* **1997**, *104*, 191–194.

(14) Xu, X. X.; Wen, Z. Y.; Wu, X. W.; Yang, X. L.; Gu, Z. H. Lithium Ion-Conducting Glass-Ceramics of $\text{Li}_{1.5}\text{Al}_{0.5}\text{Ge}_{1.5}(\text{PO}_4)_3-x\text{Li}_2\text{O}$ (x=0.0–0.2) with Good Electrical and Electrochemical Properties. *J. Am. Ceram. Soc.* **2007**, *90*, 2802–2806.

(15) Raughman, R. H.; Zakhidov, A. A.; de Heer, W. A. Carbon Nanotubes—The Route Toward Applications. *Science* **2002**, *297*, 787–792.

(16) Collins, P. G.; Bradley, K.; Ishigami, M.; Zettl, A. Extreme Oxygen Sensitivity of Electronic Properties of Carbon Nanotubes. *Science* **2000**, *287*, 1801–1804.

(17) Zhang, G. Q.; Zheng, J. P.; Liang, R.; Zhang, C.; Wang, B.; Hendrickson, M.; Plichta, E. J. Lithium–Air Batteries Using SWNT/CNT Buckpapers as Air Electrodes. *J. Electrochem. Soc.* **2010**, *157*, A953–A956.

(18) Zhang, T.; Zhou, H. S. A Reversible Long-Life Lithium–Air Battery in Ambient Air. *Nat. Commun.* **2013**, *4*, 1817.

(19) Zhang, T.; Zhou, H. S. From Li–O₂ to Li–Air Batteries: Carbon Nanotubes/Ionic Liquid Gels with a Tricontinuous Passage of Electrons, Ions, and Oxygen. *Angew. Chem., Int. Ed.* **2012**, *51*, 11062–11067.

(20) Aetukuri, N. B.; McCloskey, B. D.; Garcia, J. M.; Krupp, L. E.; Viswanathan, V.; Luntz, A. C. Solvating Additives Drive Solution-Mediated Electrochemistry and Enhance Toroid Growth in Non-Aqueous Li–O₂ Batteries. *Nat. Chem.* **2015**, *7*, 50–56.

(21) Schwenke, K. U.; Metzger, M.; Restle, T.; Piana, M.; Gasteiger, H. A. The Influence of Water and Protons on Li_2O_2 Crystal Growth in Aprotic Li–O₂ Cells. *J. Electrochem. Soc.* **2015**, *162*, A573–A584.